
Article:
Lloyd, AJ, Potter, NJ, Fishwick, CWG et al. (2013) Adenosine Tetraphosphoadenosine Drives a Continuous ATP-Release Assay for Aminoacyl-tRNA Synthetases and Other Adenylate-Forming Enzymes. ACS Chemical Biology, 8 (10). 2157 - 2163. ISSN: 1554-8937

https://doi.org/10.1021/cb400248f

Adenosine Tetraphosphoadenosine Drives a Continuous ATP-Release Assay for Aminoacyl-tRNA Synthetases and Other Adenylate-Forming Enzymes

Adrian J. Lloyd[1*#], Nicola J. Potter[2#], Colin W.G. Fishwick[2], David I. Roper[1] and Christopher G. Dowson[1*]

[1]Department of Life Sciences, University of Warwick, Gibbet Hill Road, Coventry, West Midlands, CV4 7AL, UNITED KINGDOM and [2]School of Chemistry, University of Leeds, Leeds, LS2 9JT, UNITED KINGDOM.

*To whom correspondence should be addressed: Adrian J. Lloyd email: Adrian.Lloyd@warwick.ac.uk, Tel: +44 (0)2476 522568, Fax: +44(0)2476 523568 and Christopher G. Dowson email: C.G.Dowson@warwick.ac.uk, Tel: +44 (0)2476 523534, Fax: +44(0)2476 523568.

#Both authors contributed equally to the manuscript.

Abstract

Aminoacyl-tRNA synthetases are essential for the correct linkage of an amino acid to its cognate tRNA. The accuracy of this reaction is key to the fidelity of protein synthesis. Tractable, continuous assays are of value both in characterizing the functions of these enzymes and their exploitation as drug targets. Therefore, we have exploited the hitherto unexplored ability of these enzymes to consume the diadenosine nucleotide diadenosine 5',5''' P^1 P^4 tetraphosphate (adenosine tetraphosphoadenosine (Ap_4A)) with the concomitant production of ATP in a pyrophosphate and amino acid dependent manner to develop such an assay. We have used this assay to probe the stereo-selectivity of amino acid activation by isoleucyl-$tRNA^{Ile}$ and Valyl-$tRNA^{Val}$ synthetases and to identify analogues of intermediates in their catalytic pathway that might facilitate simultaneous targeting of multiple synthetases. Finally we report the utility of Ap_4A based assays in the screening and subsequent identification of inhibitors of these enzymes, where the kinetics of Ap_4A utilization allow the detection of inhibitors with nM to mM affinities.

Introduction

The ability of small molecules to distinguish between eukaryotic and prokaryotic protein synthesis has provided the basis of antimicrobial activity for a number of clinically valuable antibiotics[1,2]. This includes the antibiotic mupirocin, which is used therapeutically as a topical agent targeting the active site of Gram positive isoleucyl-$tRNA^{Ile}$ synthetase (IleRS)[3-5], preventing the formation of isoleucyl-$tRNA^{Ile}$. However, the lack of systemic efficacy of mupirocin and its inactivity against Gram negative and TB infections[6,7] as well as the rise of mupirocin resistance in MRSA and MSSA[3,8] has increased the need for new inhibitors targeting this class of enzymes.

Many aminoacyl-tRNA synthetases (AaRSs) cannot bind the correct amino acid with sufficient accuracy to ensure the fidelity of protein synthesis[9]. Therefore these enzymes

have developed editing strategies to remove incorrectly aminoacylated intermediates and mis-aminoacylated tRNAs in what are termed pre and post-transfer editing mechanisms. These mechanisms are partitioned between the active site (pre-transfer) and a physically distinct dedicated (post-transfer) editing domain[10-14]. Recent attempts to target the interaction of $tRNA^{Leu}$ with the post-transfer editing domain of leucyl-$tRNA^{Leu}$ synthetase (LeuRS) from Gram negative pathogens with small molecule boron inhibitors have been abandoned because of the rapid onset of resistance in clinical trials due to mutation[15]. The clinical efficacy of mupirocin compared to that of small molecule boron inhibitors highlights the relative essentiality and mutability of the active site versus the post-transfer editing sites of AaRSs and consequently their value as antibacterial targets particularly where synthetases utilise more than one mechanism of editing[(16,17)]. This weakness in targeting post-transfer editing in prokaryotes is further illustrated by *Escherichia coli* LeuRS where mutation of the post-transfer editing site unveils a pre-transfer-editing capability[18].

All AaRSs share a mechanism involving activation of the cognate amino acid by reaction with ATP to form a central aminoacyl-adenylate (Figure 1). AaRSs then catalyse the attack of this central intermediate by tRNA to form the correct aminoacyl-tRNA product[14]. However, in the absence of tRNA, these enzymes can catalyse the cleavage of this central aminoacyl-adenylate by pyrophosphate. Consequently, [^{32}P]-Pyrophosphate can be employed to study pyrophosphate exchange into ATP which can be monitored as an output (Figure 1 reaction 1)[19]. Alternatively, the formation of the aminoacyl-tRNA from the aminoacyl-adenylate intermediate (Figure 1, reaction 2) can be followed in the presence of radiolabelled amino acid by trichloroacetic acid precipitation of the radiolabelled aminoacylated tRNA product[19].

However, the utilization of radiolabels can be problematic, it precludes continuous monitoring of AaRS activity and because of the costs of purchase and disposal, often precludes high throughput and saturating substrate experiments [19]. This and the success of mupirocin suggest a significant advance in inhibitor screening could be leveraged by

introduction of continuous non-radioactive assays that monitored AaRS catalysed aminoacyl adenylate turnover. Furthermore, such an assay could also be applied more generally to AaRS enzymology.

For many synthetases, the nucleophile attacking the aminoacyl-adenylate can also be the oxygen atom appended to the γ-phosphorous of a second molecule of ATP, instead of pyrophosphate or tRNA, which attacks the α-phosphorus of the adenylate moiety of the aminoacyl-adenylate. This results in the amino acid-dependent formation of Ap_4A (Figure 1, reaction 3)[20-23].

Reversal of amino acid-dependent Ap_4A formation by AaRSs, in the presence of pyrophosphate would be expected to generate two molecules of ATP which could then be detected by spectrophotometric, fluorometric or bioluminescent methodologies. This would provide a viable alternative to [^{32}P]-pyrophosphate exchange assays. Therefore, we demonstrate here that amino acid, pyrophosphate and Ap_4A dependent ATP generation can be followed continuously by tractable spectrophotometric coupled assays that can be applied to the now straightforward characterization of AaRS enzymology and for detection of inhibitors of a number of these essential drug targets.

Results and Discussion

Requirement for the generation of novel AaRS assays. We initially identified the assay partially developed by Roy[24] as a starting point. Here, the pyrophosphate nucleophile attacking the aminoacyl adenylate intermediate would exchange for the imidodiphosphate moiety of 5'-adenylyl-β,γ-imidodiphosphate (ADPNP) in the presence of the amino acid to generate ATP that could then be assayed spectrophotometrically (Supporting Information Figure 1 (Figure S1a)). This approach was flawed by the inability of Roy[24] to show dependence of the rates detected on pyrophosphate. Nevertheless we re-developed this method to obtain a working assay that was applicable to *E. coli* and *Streptococcus*

pneumoniae alanyl-tRNA^{Ala} and *S. pneumoniae* seryl-tRNA^{Ser} synthetases (AlaRS and SerRS) that we kinetically characterised (Table S1 and Figure S2a-i).

However we found this approach was limited by the inability of the class I IleRS and valyl-tRNA^{Val} synthetases (ValRS) from *E. coli* to utilise ADPNP (Figure S1b), as was also found for the baker's yeast enzymes by Friest *et al*.[25]. Furthermore, the low ADPNP K_m^{App} of *E. coli* AlaRS (4.8 ± 0.64 μM; Table S1) reduced the sensitivity of the assay to the detection of competitive inhibitors. It is possible that this restriction of adenine nucleotide specificity is related to the differential mode of ATP binding to class I and II synthetases[14,26]. To enable access to the enzymology of both class I and II AaRSs, in the context of screening for small molecule inhibitors with a high degree of sensitivity to hit detection, we sought another potential adenylate based substrate to support pyrophosphate exchange activity.

Reversal of AaRS-catalysed Ap_4A synthesis suggests an ATP release assay. All of the synthetases discussed above have been observed to synthesise Ap_4A where the aminoacyl adenylate formed with the concomitant generation of pyrophosphate, would be cleaved by a second molecule of ATP[20-22]. We investigated the reverse of this process where the synthetase would catalyse the amino acid and pyrophosphate dependent pyrophosphorolysis of Ap_4A to form two molecules of ATP that could be continuously monitored (Figure 2).

The assays based around the conversion of Ap_4A to ATP require a detection system that could distinguish between these phosphonucleotides and provide a read out of ATP in the presence of a considerable excess of Ap_4A. The ability of hexokinase to discriminate between ATP and ATP analogues such as ADPNP[24] and adenosine β methylene triphosphate (Lloyd, unpublished) was therefore tested with respect to Ap_4A. Here, phosphorylation of glucose with ATP by hexokinase was coupled to oxidation of the resulting glucose 6-phosphate to 6-phosphogluconate with reduction of $NADP^+$ by glucose 6-phosphate dehydrogenase to generate NADPH and therefore a spectrophotometric readout

at 340 nm (Figure 2). Under these circumstances, in the presence of 6.33 mM Ap_4A, no significant change in absorbance could be detected. However, on addition of 0.1 mM ATP, there was an instantaneous increase in absorbance consistent with the concentration of ATP in the assay. This suggested that the coupling system could adequately discriminate between ATP and Ap_4A and was not significantly inhibited by the dinucleotide.

We then tested the ability of *E. coli* AlaRS, *E. coli* ValRS and *E. coli* IleIRS to catalyse ATP production from Ap_4A and investigated the dependence of this process on the presence of the synthetase, the cognate amino acid and pyrophosphate. All three enzymes showed linear Ap_4A, pyrophosphate, synthetase and amino acid dependent production of ATP as an increase in absorbance at 340nm over the rate measured in the absence of any one of these components (Figure 3a-c).

To prove that the assay followed the pyrophosphorolytic cleavage of Ap_4A we followed a time course of the complete consumption of the diadenosine nucleotide by *S.pneumoniae* AlaRS in the presence of L-alanine and excess pyrophosphate. We observed that by the end point of the reaction, two equivalents of ATP were produced per equivalent of Ap_4A (Figure 3d). This was consistent with the stoichiometry of the cleavage of Ap_4A by pyrophosphate.

The reaction scheme of amino acid-dependent AaRS catalysed pyrophosphorolysis of Ap_4A indicated that the reaction would not be limited by the concentration of the amino acid which is regenerated per catalytic cycle (Figure 2). Therefore, we performed assays with IleRS at a limiting (10 μM) concentration of L-isoleucine. The absorbance of the assay at 340 nm extended beyond that expected where L-isoleucine was simply consumed (0.062 AU), to that consistent with consumption of the next limiting substrate in the assay (pyrophosphate; Figure 3c).

Characterization of AaRS Ap_4A consumption kinetics suggest an elevated sensitivity to detection of inhibitors. Having established that IleRS, ValRS and AlaRS catalysed the pyrophosphorolysis of Ap_4A to two equivalents of ATP, we characterised the kinetics of L-amino acid, pyrophosphate and Ap_4A utilization by *E. coli* IleRS, ValRS and AlaRS. For all three enzymes, dependence of activity on Ap_4A, amino acid and pyrophosphate was strictly hyperbolic (Figure S3a-i). Fitting the data to the Michaelis Menten equation generated the kinetic constants for the dependence of activity of these enzymes on their substrates in the Ap_4A assay (Table 1).

Comparison of ADPNP and Ap_4A based assays (Tables 1 and S1, Figures S2h and S3h) revealed that for the *E. coli* AlaRS, the K_m^{App} for Ap_4A (0.87 ± 0.17 mM) was 181-fold greater than that for ADPNP (4.8 ± 0.64 μM). Comparison of the data in Table 1 and Figure S3h, S3b and S3e with previous ^{32}P-pyrophosphate exchange measurements with cognate amino acids suggested that the K_m^{App} of *E. coli* AlaRS, IleRS and ValRS for Ap_4A was 16.8-fold[27], 45.2-fold[28] and 19.4-fold[29] greater than for ATP. This suggested that Ap_4A utilization afforded the convenience of a continuous non-radioactive assay, and also endowed synthetase assays with kinetic constants that would be more sensitive to inhibitor detection than if assays utilised ATP as the adenylate substrate.

The data in Table 1 and Figure S3f and i also demonstrate that the K_m^{App} values in the Ap_4A assay for the cognate amino acids for ValRS and AlaRS were in the high millimolar range (14.22 ± 1.54 mM and 12.64 ± 1.86 mM respectively) where previously, values in the ATP/pyrophosphate exchange reaction were 0.14 mM[30] and 0.18 mM[27]. The increase in the IleRS K_m^{App} for L-isoleucine in the Ap_4A assay (37.04 ± 3.17 μM; Table 1, Figure S3c) relative to that previously published (4 μM[31]); was less marked, but nevertheless significant. The 101-fold, 70.2-fold and 9.26-fold increase in amino acid K_m^{App} for the ValRS, AlaRS and IleRS respectively may have resulted from a reduced affinity of the amino acid for synthetases bound to Ap_4A. Similarly as concluded from the dependence of rates on Ap_4A,

the sensitivity of assays to the detection of amino acid or aminoacyl-adenylate synthetase-targeted inhibitors would be expected to be vastly enhanced by the relatively high K_m^{App} values shown by these enzymes for their cognate amino acids.

The Ap_4A assay applied to analysis of AaRS chemical and stereochemical amino acid specificity. ValRS[32], IleRS[32] and AlaRS[33] form adenylates and aminoacyl-tRNA species with non-cognate amino acids. We therefore tested the ability of these enzymes to utilise Ap_4A as a substrate with L-threonine, L-serine and L-valine, the respective non-cognate editing substrates of these enzymes[32,33].

The Ap_4A-activation of L-valine by IleRS and L-serine by *S. pneumoniae* AlaRS was easily detectable (Figure 4 and Figure S4). Here, the efficiencies reported by relative k_{cat}^{App}/K_m^{App} values of L-valine and L-isoleucine activation by *E. coli* IleRS (Table 1) were 1:206.3 which is in excellent agreement with previous measurement of 1:200 for this parameter using ^{32}P-pyrophosphate exchange[34] and consistent with the requirement of editing mechanisms by IleRS. However, consumption of Ap_4A by ValRS was barely detectable in the presence of 15 mM of its non-cognate L-threonine substrate. It is probable that the impact of a reduced affinity for both non-cognate amino acid and the substitution of ATP by Ap_4A on catalysis was sufficient to severely reduce observable ValRS activity.

The utilization of Ap_4A by IleRS and ValRS allowed us to extend our studies to the utilization of D-isoleucine and D-valine by these enzymes. In this assay, D-valine did not support ValRS activity, consistent with the previously noted stereo-specificity of this enzyme[35,36]. Similarly, D-valine was not subject to non-cognate activation by IleRS, again, consistent with previous observations[37].

In contrast, D-isoleucine was activated by IleRS in the presence of Ap_4A (Figure 4). Comparison of relative efficiencies of activation suggested that IleRS was only 185.4-fold more efficient with L-isoleucine as opposed to D-isoleucine, caused principally by a 110.5-

fold increase in K_m^{App} (Table 1). This level of discrimination is similar to that between L-isoleucine and L-valine which has required the evolution of both post and pre-transfer editing domains to eliminate erroneous incorporation of L-valine at L-isoleucine codons[9-14,32,34]. Previous attempts[37] to demonstrate D-isoleucine utilization by IleRS were not successful, however, these assays were performed with a limit of detection of $\geq$1% the rate with cognate L-isoleucine[37], and as we have demonstrated here, although significant, the efficiency of the enzyme with D-isoleucine is less than ~0.5% of that with L-isoleucine.

How mis-activation of D-isoleucine by IleRS is subsequently dealt with is of current interest, as this D-amino acid and others are found naturally in the peptidoglycan of stationary phase bacterial cultures[38]. This raises the possibility that formation of D-isoleucyl-$tRNA^{Ile}$ may challenge the stereochemical fidelity of protein synthesis, a possibility made more likely by our inability to demonstrate any editing activity with respect to D-isoleucine utilization by *E. coli* IleRS (Lloyd unpublished data).

Aminoacyl-adenylate mimetics suggest a possible multi-targeted approach to inhibition of AaRSs. To further validate the Ap_4A assay, we used a series of standard synthetase inhibitors that mimic the aminoacyl-adenylate intermediates of AaRS activity (Figure 5). Mupirocin acts as a tight binding analogue of isoleucyl-adenylate[3-5]. In the Ap_4A assay, mupirocin was a potent IleRS inhibitor (Figure 3c) with an IC_{50} of 0.35 ± 0.06 µM (Figure 5a) approximating to half the concentration of IleRS (1.13 µM) confirming the tight-binding nature of this inhibitor. Conversely, mupirocin was a weak ValRS inhibitor (37% at 0.5 mM), consistent with the specificity of the drug towards prokaryotic IleRS.

The aminoacyl-5'-sulphamoyl adenosines are potent AaRS inhibitors[39] and *E. coli* AlaRS was inhibited by alanyl-5'-sulphamoyl adenosine (Figure 3a) with an IC_{50} of 0.403 ± 0.005 µM (Figure 5b). The impact of cognate adenylate analogues on their cognate AaRSs as shown here with AlaRS and IleRS confirmed the utility of the Ap_4A assay. It is known that ten of the AaRSs mis-activate non-cognate amino acids to their corresponding adenylates

and require editing mechanisms to preserve the genetic code[9,11,13]. This suggested that if the same amino acid was mis-activated by multiple synthetases, then a non-hydrolysable mimic of its aminoacyl-adenylate may target these AaRSs as well as its cognate synthetase.

L-Threonine is mis-activated by ValRS which has editing mechanisms preventing the mis-threonylation of $tRNA^{Val\ 32}$. We therefore surmised that ValRS might be inhibited by the non-cognate adenylate analogue threonyl-5'-sulphamoyl adenosine. This indeed was the case (Figure 3b) and we further found in the Ap_4A assay that ValRS was inhibited by this compound with an IC_{50} of 6.82 ± 0.77 μM (Figure 5c). This suggested threonyl-5'-sulphamoyl adenosine could multiply target noncognate ValRS and cognate ThrRS. This was confirmed with the ADPNP/pyrophosphate exchange assay which showed that threonyl-5'-sulphamoyl adenosine inhibited *S. pneumoniae* ThrRS with an IC_{50} of 0.175 ± 0.019 μM (Figure 5c). The 38-fold greater potency of threonyl-5'-sulphamoyl adenosine towards ThrRS relative to ValRS is likely to mirror at least in part the substrate specificities of these two synthetases.

To further investigate the multi-targeting of AaRSs, we explored the inhibitory properties of the seryl-adenylate analogue seryl-5'-sulphamoyl adenosine. Seryl-adenylate is formed by the adenylation of L-serine by SerRS, and mis-adenylation by AlaRS and ThrRS[14,33,40]. Using the *S. pneumoniae* enzymes we showed that (a) SerRS was inhibited by seryl-5'-sulphamoyl adenosine with an IC_{50} of 0.44 ± 0.076 μM (Figure 5d); (b) AlaRS was inhibited with an IC_{50} of 0.133 ± 0.046 μM (Figure 5d) and (c) ThrRS was inhibited with an IC_{50} of between 5 and 50 μM (Figure S5a). Interestingly, alanyl-5'-sulphamoyl adenosine was not an inhibitor of SerRS (Figure S5b), consistent with the requirement by this enzyme for the β-hydroxyl of L-serine for amino acid recognition[23]. None of these inhibitors affected the activity of the hexokinase/glucose 6 phosphate dehydrogenase coupling system.

Interestingly, the overlapping potency of the above aminoacyl adenylate mimetics are consistent with the overlapping amino acid substrate specificity of these three

synthetases[9,11,13,33,40] and may explain the extremely high potency of sideromycins such as albomycin, a natural pro-drug antibiotic that releases a cleavable warhead comprising a seryl adenylate analogue[41] on entry into the target bacterial cell. Our data suggest that this warhead could simultaneously deprive protein synthesis of seryl-tRNA^{Ser}, alanyl-tRNA^{Ala} and threonyl-tRNA^{Thr}.

Our data suggest that multiple AaRSs that share the formation of a cognate or non-cognate aminoacyl adenylates could be targeted by a single inhibitor. Indeed, alanyl-5' sulphamoyl adenosine is a nanomolar inhibitor of not only AlaRS but also of *E. coli* prolyl-tRNA^{Pro} synthetase[42]. Multi-targeting of a molecule to multiple essential gene products is attractive for antimicrobial development because of the additional hurdles it presents to the development of resistance[43]. Therefore, development of multi-targeted AaRS inhibitors using for example seryl-adenylate analogues as a starting point may allow development of novel antimicrobials which are robust with respect to the evolution of resistance.

Assessment of the Ap_4A assay in the screening for AaRS inhibitors. The original motivation for the development of the Ap_4A assay was to assess the inhibitory properties of molecules selected or designed as a result of *in silico* drug design. This required an assay whose sensitivity to competitive inhibitors was enhanced by virtue of utilization of substrates that possessed a low affinity for the enzyme.

We employed *in silico* drug design by SPROUT[44] to identify small molecules that could bind to the aminoacyl-adenylate binding pockets of both *E. coli* IleRS and ValRS. Cognisant of our Ap_4A kinetic data regarding the substrate dependences of these synthetases, we configured assays at sub-saturating amino acid and Ap_4A concentrations to optimise the sensitivity of the assay to inhibitors competitive with respect to the amino acid, ATP and aminoacyl-adenylate binding sites. For IleRS these were (Concentration/ Concentration relative to K_m^{App}) Ap_4A: 0.7 mM/0.11.K_m^{App}, L-isoleucine: 10 μM/0.27.K_m^{App} and pyrophosphate: 20 μM/6.43.K_m^{App}. Similarly, for ValRS these were Ap_4A: 0.388

mM/0.20.K_m^{App}, L-valine: 4 mM/0.32.K_m^{App} and pyrophosphate: 20 μM/8.23.K_m^{App}. Typical rates measured under these circumstances for both enzymes are shown in Figure 3b,c.

Under these conditions, the standard deviation of the assays for both enzymes expressed as a percentage of the mean value for a triplicate determination of initial rate was 7.0 % (range, 2.4% - 9.2% n = 7) for IleRS and 4.8 % (range, 1.7% - 8.1% n = 10) for ValRS. Assuming a positive identification of an inhibitor was a drop in measured activity of at least three standard deviations and competitive kinetics, these assays would detect IleRS inhibitors competitive with L-isoleucine, Ap_4A and pyrophosphate with K_i values ≤ 3.0 mM, ≤ 3.4 mM and ≤ 0.51 mM respectively at a set inhibitor concentration of 1 mM. Similarly, ValRS inhibitors competitive with L-valine, Ap4A and pyrophosphate with K_i values ≤ 4.5 mM, ≤ 5.0 mM and ≤ 0.43 mM respectively would be expected to be detected.

We assessed the signal:noise ratio of the assay (the ratio of rates with and without pyrophosphate). For IleRS and ValRS, the signal to noise ratios of the assays at the concentration of the enzyme used in screening (2.25 μM and 2.21 μM respectively) were 3.86 ± 1.15 (n= 35 positive controls) and 7.79 ± 2.14 (n = 30 positive controls) respectively.

We further characterised the ability of the assay to discriminate between the presence and absence of standard inhibitors. The Z' values[45] for the IleRS assay with respect to inhibition by 5 μM mupirocin and the ValRS assay with respect to inhibition by 50 μM threonyl-5'-sulphamoyl adenosine were 0.84 and 0.792, suggesting excellent discrimination between positive and negative control assays.

With the assay thus configured, we screened a library of 73 compounds against both enzymes. Although we were unable to identify novel dual targeted inhibitors in this manner, we identified two IleRS inhibitors: N-tert-Butyl-2-(3-{[3-(tert-butylcarbamoyl-methyl)benzyl-amino]-methyl}-phenyl)-acetamide (195) and N-Isopropyl-2-(3-{[3-(isopropyl-carbamoyl-methyl)-benzylamino]-methyl}-phenyl)-acetamide (202) exerting 82.2 and 75.3% inhibition at

1 mM with Z-factors of 0.73 and 0.55 and IC_{50} values on re-screening of 0.22 ± 0.035 mM and 0.895 ±0.057 mM respectively (Figure 6a and b). These molecules exerted no effect on the hexokinase/6-phospho-gluconate dehydrogenase coupling system, nor were they inhibitors of ValRS.

Both 195 and 202 were competitive inhibitors against L-isoleucine and Ap_4A with K_i values for 195 vs Ap_4A and L-isoleucine of 0.14 and 0.184 mM respectively and for 202 vs Ap_4A and L-isoleucine of 0.792 and 0.398 mM respectively (Figures 6c-f). This suggested that they bound to IleRS at the site they were targeted to (Figures 6c-f). The K_i values suggested weak binding for these inhibitors to IleRS, compared to the inhibitors already discussed, but are consistent with the starting point for fragment based drug design[46].

Screening of this library with ValRS identified HTS026477 (4-Amino-2-[2-oxo-2-(3-phenyl-isoxazol-5-yl)ethylsulfanyl]-pyrimidine-5-carboxylic acid)) that was not an IleRS inhibitor. This molecule exerted 62.8% inhibition (Z' factor = 0.74) and on re-screening displayed a sigmoid dependence of inhibition on concentration (IC_{50} = 1.51 ± 0.32 mM, Hill coefficient of 3.65 ± 0.68; Figure 7d)). Although we did not characterise the interaction of HTS026477 with ValRS further, to gain additional insight into molecules that might bring about inhibition of this enzyme, we identified a series of triazinyl dyes that inhibited the enzyme, based on our and previous observations regarding ValRS purification with immobilised dyes[47]. These dyes were Procion Red HE-3B, Procion Green HE4BD and Trypan Blue. IC_{50} values for these compounds were 2.14 ± 0.29 μM, 6.98 ± 1.23 μM and 19.2 ± 8.6 μM respectively (Figures 7a-c).

Interestingly, Procion Green HE4BD inhibits *Bacillus stearothermophilus* methionyl-$tRNA^{Met}$ synthetase[48] suggesting that this dye could provide a starting point for the development of multi-targeted AaRS inhibitors. Trypan blue has anti-trypanosomal activity, targeting the glycolytic pathway[49] and is used in the treatment of trypanosomiasis. Our data

suggest that this molecule may also interfere with protein synthesis by targeting ValRS, which itself may be a viable strategy in treatment of this disease.

These data highlight the capability of Ap_4A based assays to analyse binding events to synthetases from nM to mM affinities and exemplify the utility of this assay in fundamental and translational AaRS research.

Finally, the potential utility of this assay is greater than that reported here. Many drug targets turnover Ap_4A, and we are currently pursuing assay development for these enzymes[50]. Furthermore, NADPH utilization as a reporter of enzyme activity suggests an additional fluorescence format for these assays, whilst the exploitation of Ap_4A to generate ATP indicates the potential for linking Ap_4A consumption to a fire-fly luciferase based luminescence readout.

Methods

E. coli AlaRS, IleRS, and ValRS and *S. pneumoniae* AlaRS, SerRS, and ThrRS were expressed as C-terminal hexahistidine fusion proteins and were purified as described[51]. Purification of ValRS was completed by chromatography on Sepharose-4B coupled to Procion Green HE4BD to eliminate contamination with inorganic pyrophosphatase. *Leuconostoc mesenteroides* glucose 6 phosphate dehydrogenase and yeast hexokinase were obtained from Roche. Alanyl-, threonyl and seryl-5'-sulphamoyl adenosines were from IDT, Ap_4A was from Sigma. All other reagents were from Sigma or Melford.

AaRS assays were performed at 37ºC in a Cary 100 UV/Vis double beam spectrophotometer with a thermostatted 6X6 cell changer. The final assay volume was 0.2 ml, containing 50 mM HEPES adjusted to pH 7.6, 10 mM $MgCl_2$, 50 mM KCl, 1 mM dithiothreitol, 10% (v/v) dimethylsulphoxide, 10 mM D-glucose, 0.5 mM $NADP^+$, 1.7 mM.min *L. mesenteroides* hexokinase and 0.85 mM.min *L. mesenteroides* glucose 6-phosphate dehydrogenase. Concentrations of AaRS, amino acid, adenylate (Ap_4A or ADPNP) and

pyrophosphate were as stated in the text. Unless otherwise stated, background rates were acquired in the absence of pyrophosphate, which was then added to initiate the full reaction. Assays were continuously monitored at 340 nm, to detect reduction of $NADP^+$ to NADPH, where $\varepsilon_{NADPH;\ 340nm} = 6220\ M^{-1}.cm^{-1}$.

Kinetic constants relating to substrate dependencies and IC_{50} values for inhibitors were extracted by non-linear regression using GraphPad Prizm. Modes of inhibition and K_i values were evaluated by linear regression of dependencies of reciprocal velocity on reciprocal substrate concentration at varying inhibitor concentration.

Acknowledgments

We would like to thank the MRC for financial support. A.J. Lloyd is a Science City Interdisciplinary Research Alliance Research Fellow, supported by the Birmingham-Warwick Science City Translational Medicine Initiative.

References

1: Sutcliffe, J. A. (2011) Antibiotics in development targeting protein synthesis. *Ann. N. Y. Acad. Sci.* 1241, 122-152.

2. Walsh, C. (2003) Where will the new antibiotics come from? *Nat. Rev. Microbiol.* 1, 65-70.

3: Hurdle, J. G., O'Neill, A. J., and Chopra, I. (2005) Prospects for aminoacyl-tRNA synthetase inhibitors as new antimicrobial agents. *Antimicrob. Agents Chemother.* 49, 4821-4833.

4: Silvian, L. F., Wang, J., and Steitz, T. A. (1999) Insights into editing from an ile-tRNA synthetase structure with $tRNA^{ile}$ and mupirocin. *Science* 285, 1074-1077.

5: Nakama, T., Nureki, O., and Yokoyama, S. (2001) Structural basis for the recognition of isoleucyl-adenylate and an antibiotic, mupirocin, by isoleucyl-tRNA synthetase. *J. Biol. Chem.* 276, 47387-47393.

6: Sassanfar, M., Kranz, J. E., Gallant, P., Schimmel, P., and Shiba, K. (1996) A eubacterial *Mycobacterium tuberculosis* tRNA synthetase is eukaryote-like and resistant to a eubacterial-specific antisynthetase drug. *Biochemistry* 35, 9995-10003.

7: Sutherland, R., Boon, R. J., Griffin, K. E., Masters, P. J., Slocombe, B., and White, A. R. (1985) Antibacterial activity of mupirocin (pseudomonic acid), a new antibiotic for topical use. *Antimicrob. Agents Chemother*. 27, 495-498.

8: Patel, J. B., Gorwitz, R. J., and Jernigan, J. A. (2009) Mupirocin resistance. *Clin. Infect. Dis.* 49, 935-941.

9: Yadavalli, S. S., and Ibba, M. (2012) Quality control in aminoacyl-tRNA synthesis its role in translational fidelity. *Adv. Protein Chem. Struct. Biol*. 86, 1-43.

10: Reynolds, N. M., Lazazzera, B. A., and Ibba, M. (2010) Cellular mechanisms that control mistranslation. *Nat. Rev. Microbiol.* 8, 849-856.

11: Jakubowski, H. (2012) Quality control in tRNA charging. *Wiley Interdiscip. Rev. RNA* 3, 295-310.

12: Martinis, S. A., and Boniecki, M. T. (2010) The balance between pre- and post-transfer editing in tRNA synthetases. *FEBS Lett.* 584, 455-459.

13: Ling, J., Reynolds, N., and Ibba, M. (2009) Aminoacyl-tRNA synthesis and translational quality control. *Annu. Rev. Microbiol.* 63, 61-78.

14: Ibba, M, and Söll, D. (2000) Aminoacyl-tRNA synthesis. *Annu. Rev. Biochem.* 69, 617-50.

15: Hernandez, V., Crépin, T., Palencia, A., Cusack, S., Akama, T., Baker, S. J., Bu, W., Feng, L., Freund, Y. R., Liu, L., Meewan, M., Mohan, M., Mao, W., Rock, F. L., Sexton, H., Sheoran, A., Zhang, Y., Zhang, Y. K., Zhou, Y., Nieman, J. A., Anugula, M. R., Keramane, E. M., Savariraj, K., Reddy, D. S., Sharma, R., Subedi,

R., Singh, R., O'Leary, A., Simon, N. L., De Marsh, P. L., Mushtaq, S., Warner, M., Livermore, D. M., Alley, M. R., and Plattner, J. J. (2013) Discovery of a Novel Class of Boron-based Antibacterials with Activity against Gram-negative Bacteria. *Antimicrob. Agents Chemother.* 57, 1394-1403.

16: Cvetesic, N., Perona, J. J., and Gruic-Sovulj, I. (2012) Kinetic partitioning between synthetic and editing pathways in class I aminoacyl-tRNA synthetases occurs at both pre-transfer and post-transfer hydrolytic steps. *J. Biol. Chem.* 287, 25381-25394.

17: Splan, K. E., Ignatov, M. E., and Musier-Forsyth, K. (2008) Transfer RNA modulates the editing mechanism used by class II prolyl-tRNA synthetase. *J. Biol. Chem.* 283, 7128-7134.

18: Williams, A. M., and Martinis, S. A. (2006) Mutational unmasking of a tRNA-dependent pathway for preventing genetic code ambiguity. *Proc. Natl. Acad. Sci. U S A.* 103, 3586-3591.

19: Francklyn, C. S., First, E. A., Perona, J. J., and Hou, Y. M. (2008) Methods for kinetic and thermodynamic analysis of aminoacyl-tRNA synthetases. *Methods* 44, 100-118.

20: Zamecnik, P. (1983) Diadenosine 5',5"'-P1,P4-tetraphosphate (Ap4A): its role in cellular metabolism. *Anal. Biochem.* 134, 1-10.

21: Goerlich, O., Foeckler, R., and Holler, E. (1982) Mechanism of synthesis of adenosine(5') tetraphospho(5')adenosine (AppppA) by aminoacyl-tRNA synthetases. *Eur. J. Biochem*. 126, 135-142.

22: Blanquet, S., Plateau, P., and Brevet, A. (1983) The role of zinc in 5',5'-diadenosine tetraphosphate production by aminoacyl-transfer RNA synthetases. *Mol. Cell. Biochem.* 52, 3-11.

23: Belrhali, H., Yaremchuk, A., Tukalo, M., Berthet-Colominas, C., Rasmussen, B., Bösecke, P., Diat, O., and Cusack, S. (1995) The structural basis for seryl-adenylate and Ap4A synthesis by seryl-tRNA synthetase. *Structure* 3, 341-352.

24: Roy, S. (1983) A continuous spectrophotometric assay for *Escherichia coli* alanyl-transfer RNA synthetase. *Anal. Biochem.* 133, 292-295.

25: Freist, W., Wiedner, H., and Cramer, F. (1980) Chemically modified ATP derivatives for the study of aminoacyl-tRNA synthetases from baker's yeast: ATP analogs with fixed conformations or modified triphosphate chains in the aminoacylation reaction. *Bioorg. Chem.* 9, 491-504.

26: First, E. A. (2005) catalysis of the tRNA aminoacylation reaction. In *The aminoacyl-tRNA synthetases* (Ibba, M., Francklyn, C., and Cusack, S. Eds.) Chp. 30, pp 328-352, Landes Bioscience, Texas, USA.

27: Davis, M. W., Buechter, D. D., and Schimmel, P. (1994) Functional dissection of a predicted class-defining motif in a class II tRNA synthetase of unknown structure. *Biochemistry* 33, 9904-9911.

28: Yanagisawa, T., Lee, J. T., Wu, H. C., and Kawakami, M. (1994) Relationship of protein structure of isoleucyl-tRNA synthetase with pseudomonic acid resistance of *Escherichia coli.* A proposed mode of action of pseudomonic acid as an inhibitor of isoleucyl-tRNA synthetase. *J. Biol. Chem.* 269, 24304-24309.

29: Myers, G., Blank, H. U., and Söll, D. (1971) A comparative study of the interactions of *Escherichia coli* leucyl-, seryl-, and valyl-transfer ribonucleic acid synthetases with their cognate transfer ribonucleic acids. *J. Biol. Chem.* 246, 4955-4964.

30: Owens, S. L., and Bell, F. E. (1970) Specificity of the valyl ribonucleic acid synthetase from *Escherichia coli* in the binding of valine analogues. *J. Biol. Chem.* 245, 5515-5523.

31: Fersht, A. R. (1977) Editing mechanisms in protein synthesis. Rejection of valine by the isoleucyl-tRNA synthetase. *Biochemistry* 16, 1025-1030.

32: Dulic, M., Cvetesic, N., Perona, J. J., and Gruic-Sovulj, I. (2010) Partitioning of tRNA-dependent editing between pre- and post-transfer pathways in class I aminoacyl-tRNA synthetases. *J. Biol. Chem.* 285, 23799-23809.

33: Beebe, K., Ribas De Pouplana L., and Schimmel, P. (2003) Elucidation of tRNA-dependent editing by a class II tRNA synthetase and significance for cell viability. *EMBO J.* 22, 668-675.

34: Schmidt, E., and Schimmel, P. (1994) Mutational isolation of a sieve for editing in a transfer RNA synthetase. *Science* 264, 265-267.

35: Kakitani, M., Tonomura, B., and Hiromi, K. (1987) Fluorometric study on the interaction of amino acids and ATP with valyl-tRNA synthetase from *Bacillus stearothermophilus*. *J. Biochem.* 101, 477-484.

36: Owens, S. L., and Bell, F. E. (1968) Stereospecificity of the *Escherichia coli* valyl-RNA synthetase in the ATP- ^{32}PPi exchange reaction. *J. Mol. Biol.* 38, 145-146.

37: Bergmann, F. H., Berg, P., and Dieckmann, M. (1961) The enzymic synthesis of amino acyl derivatives of ribonucleic acid: II. The preparation of leucyl-, valyl-, isoleucyl- and methionyl ribonucleic acid synthetases from *Escherichia coli. J. Biol. Chem.* 236, 1735–1740.

38: Cava, F., de Pedro, M. A., Lam, H., Davis, B. M., and Waldor, M. K. (2011) Distinct pathways for modification of the bacterial cell wall by non-canonical D-amino acids. *EMBO J.* 30, 3442-3453.

39: Vondenhoff, G. H., and Van Aerschot, A. (2011) Aminoacyl-tRNA synthetase inhibitors as potential antibiotics. *Eur. J. Med. Chem.* 46, 5227-5236.

40: Minajigi, A., and Francklyn, C. S. (2010) Aminoacyl transfer rate dictates choice of editing pathway in threonyl-tRNA synthetase. *J. Biol. Chem*. 285, 23810-23817.

41: Braun, V., Pramanik, A., Gwinner, T., Köberle, M., and Bohn, E. (2009) Sideromycins: tools and antibiotics. *Biometals* 22, 3-13.

42: Hati, S., Ziervogel, B., Sternjohn, J., Wong, F. C., Nagan, M. C., Rosen, A. E., Siliciano, P. G., Chihade, J. W., and Musier-Forsyth, K. (2006) Pre-transfer editing by class II prolyl- RNA synthetase: role of aminoacylation active site in "selective release" of noncognate amino acids. *J. Biol. Chem.* 281, 27862-27872.

43: East, S. P., and Silver, L. L. (2013) Multitarget ligands in antibacterial research: progress and opportunities. *Expert Opin. Drug Discov*. 8, 143-156.

44: Gillet, V. J., Newell, W., Mata, P., Myatt, G., Sike, S., Zsoldos, Z., and Johnson, A. P. (1994) SPROUT: recent developments in the *de novo* design of molecules. *J. Chem. Inf. Comput. Sci.* 34, 207-217.

45: Iversen, P. W., Eastwood, B. J., Sittampalam, G. S., and Cox, K. L. (2006) A comparison of assay performance measures in screening assays: signal window, Z' factor, and assay variability ratio. *J. Biomol. Screen.* 11, 247-252.

46: Leach, A. R., and Hann, M. M. (2011) Molecular complexity and fragment-based drug discovery: ten years on. *Curr. Opin. Chem. Biol.* 15, 489-496.

47: Bruton, C. J., and Atkinson, T. (1979) The binding of aminoacyl-tRNA synthetases to triazine dye conjugates. *Nucleic Acids Res.* 7, 1579-1591.

48: McArdell, J. E., Duffield, M., and Atkinson, T. (1989) Probing the substrate-binding sites of aminoacyl-tRNA synthetases with the procion dye green HE-4BD. *Biochem. J.* 258, 715-721.

49: Morgan, H. P., McNae, I. W., Nowicki, M. W., Zhong, W., Michels, P. A., Auld, D. S., Fothergill-Gilmore, L. A., and Walkinshaw, M. D. (2011) The trypanocidal drug suramin and other trypan blue mimetics are inhibitors of pyruvate kinases and bind to the adenosine site. *J. Biol. Chem*. 286, 31232-31240.

50: Fraga, H., and Fontes, R. (2011) Enzymatic synthesis of mono and dinucleoside polyphosphates. *Biochim. Biophys. Acta*. 1810, 1195-1204.

51: Lloyd, A. J., Gilbey, A. M., Blewett, A. M., De Pascale, G., El Zoeiby, A., Levesque R. C., Catherwood, A. C., Tomasz, A., Bugg, T. D., Roper, D. I., and Dowson, C. G.

(2008) Characterization of tRNA-dependent peptide bond formation by MurM in the synthesis of *Streptococcus pneumoniae* peptidoglycan. *J. Biol. Chem.* 283, 6402-6417.

Table Legends

Table 1: Characterization of the kinetics of substrate dependence of E. coli AlaRS, IleRS and ValRS on the rate of pyrophosphorolysis of Ap_4A

Figure Legends

Figure 1. Catalytic activities of AaRSs. Formation of the central aminoacyl-adenylate intermediate and inorganic pyrophosphate from ATP and an amino acid[14], and reactions of this intermediate with the C-2 or C-3 hydroxyl of the 3' ribose of the cognate tRNA (reaction 2) forms an aminoacyl-tRNA. In the absence of tRNA the adenylate intermediate can be cleaved by an alternative nucleophile which can be pyrophosphate (reaction 1) which attacks the α-phosphorus atom of the aminoacyl adenylate displacing the amino acid and regenerating ATP, or the oxygen atom appended to the γ-phosphorus of a second molecule of ATP which attacks the α-phosphorus of the adenylate moiety of the aminoacyl adenylate (reaction 3). This results in the amino acid-dependent formation of diadenosine 5',5''' P^1 P^4 tetraphosphate (adenosine tetraphospho-adenosine (Ap_4A)).

Figure 2. Reversal of Ap_4A synthesis by AaRS. Cleavage of Ap_4A by an amino acid substrate and pyrophosphate yielding two molecules of ATP which can be continuously monitored by coupling to $NADP^+$ reduction to NADPH.

Figure 3: Time courses of AaRS-catalysed amino acid dependent pyrophosphorolysis of Ap_4A to ATP. PPi denotes pyrophosphate. Background rates were followed before addition of the missing component of the assay at arrow. **Panel (a)**: *E. coli* AlaRS activity, in the presence of 0.41 mM Ap_4A, 2 mM L-alanine, 20 μM

pyrophosphate and 0.92 μM AlaRS; **Panel (b)** *E. coli* ValRS activity, in the presence of 0.388 mM Ap_4A, 4 mM L-valine, 20 μM pyrophosphate and 2.41 μM ValRS; **Panel (c)** *E. coli* IleRS activity, in the presence of 0.7 mM Ap_4A, 10 μM L-isoleucine, 20 μM pyrophosphate and 2.4 μM ValRS. For **panels (a) - (c)** assays were run without (maroon trace, DMSO control) or with 5 μM alanyl-5'-sulphamoyl adenosine (ASA), 50 μM threonyl-5'-sulphamoyl adenosine (TSA) or 5 μM mupirocin (blue trace). **Panel (d)**: Stoichiometry of conversion of Ap_4A to ATP in the presence of L-alanine and *S. pneumoniae* AlaRS. Reaction was allowed to approach equilibrium in the presence of 1.8 μM AlaRS, 0.471 mM pyrophosphate and 27.2 μM Ap_4A. Final [ATP] inferred from the ΔA_{340} on completion of the reaction was 59.2 μM, implying conversion of Ap_4A to 2.16 equivalents of ATP.

Figure 4: Impact of chemical and stereochemical identity on the dependence of initial rate of IleRS on amino acid substrate. Assays were performed at co-substrate and enzyme concentrations recorded in Table 1. Data were fitted to the Michaelis Menten equation using GraphPad Prizm yielding the kinetic constants shown in Table 1.

Figure 5: Validation of the Ap_4A AaRS assay and identification of single and multiply targeted aminoacyl adenylate analogue inhibitors. **Panel (a)**: Dependence of inhibition of IleRS on mupirocin in the presence of 1.13 μM IleRS, 2 mM Ap_4A, 14.4 mM L-isoleucine and 0.471 mM pyrophosphate; **Panel (b)**: Dependence of inhibition of *E. coli* AlaRS on alanyl-5'-sulphamoyl adenosine, conditions as described in the Figure 3a; **Panel (c)**: Dependence of inhibition of *E. coli* ValRS and *S. pneumoniae* threonyl-$tRNA^{Thr}$ synthetase (ThrRS) on threonyl-5'-sulfamoyl adenosine where 1.14 μM ValRS was assayed in the presence of 2 mM Ap_4A, 14.4 mM L-valine and 0.471 mM pyrophosphate (rust) and 0.132 μM ThrRS was assayed as described for assays containing Ap_4A except 0.5 mM ADPNP was substituted for Ap_4A and L-

threonine and pyrophosphate were10 mM and 0.118 mM respectively (dark blue); **Panel (d)**:, Dependence of inhibition of *S. pneumoniae* AlaRS and SerRS on seryl-5'-sulfamoyl adenosine, where for both enzymes ADPNP and pyrophosphate were 0.25 mM and 0.471 mM respectively, and assays contained either 2.08 μM SerRS and 0.2 mM L-serine (blue) or 0.21 μM AlaRS, and 0.2 mM L-alanine (rust). Inhibitor structures are in pale yellow boxes.

Figure 6: Evaluation of the inhibitory properties of compounds 195 and 202, IleRS inhibitors identified by screening with the Ap_4A assay. All data were collected at 3.14 μM IleRS. **Panels (a)** and **(b)** show dependence of inhibition of IleRS on either compound 195 or 202 respectively. [Ap_4A], [L-isoleucine] and [pyrophosphate] were 0.7 mM, 10 μM, and 20 μM respectively. **Panels (c)** and **(d)** are reciprocal plots of IleRS activity at increasing concentrations of L-isoleucine in the presence of 0-3 mM195 **(c)** or 0-3.6 mM 202 **(d)**. **Panels (e)** and **(f)** are reciprocal plots of IleRS activity at increasing concentrations of Ap_4A in the presence of the same range of 195 **(e)** or 202 concentrations **(f)**. [Pyrophosphate] in assays contributing to data in **Panels (c)** to **(f)** was 20 μM. Inserts in panels **(c)** to **(f)** are secondary plots of slopes of reciprocal plots vs. [inhibitor]. K_i values were determined from the abscissa intercept of secondary plots.

Figure 7: Characterization of ValRS inhibitors identified by the Ap_4A assay: [ValRS], [Ap_4A], [pyrophosphate] and [L-valine] were 2.21 μM, 0.388 mM, 32 μM and: 4 mM respectively. Inhibition of ValRS by: **Panel (a)** Procion Red HE3B; **Panel (b)** Procion Green HE4BD; **Panel (c)** Trypan Blue and; **Panel (d)** HTS 02677. None of these compounds significantly inhibited IleRS, nor exerted significant inhibition of the hexokinase/6phosphogluconate dehydrogenase coupling system.

Table 1

AaRS	$[AaRS]_{Assay}$	Nonvaried substrate	[Nonvaried substrate] (mM)	Varied Substrate	K_m^{App} (μM)	k_{cat}^{App} (min^{-1})	k_{cat}^{App}/K_m^{App} ($min^{-1}.\mu M^{-1}$)
AlaRS	0.92 μM	L-Alanine	10.00	L-Alanine	14220 ± 1540	39.3 ± 1.93	0.0028
	0.92 μM	Ap_4A	3.99	Ap_4A	871 ± 171	21.85 ± 1.16	0.0251
	0.92 μM	PPi	0.471	PPi	12.81 ± 1.62	19.62 ± 0.79	1.531
IleRS	1.13 μM	L-Isoleucine	14.4	L-Isoleucine	37.04 ± 3.17	6.99 ± 0.18	0.1887
	1.13 μM	Ap_4A	5.00	Ap_4A	6330 ± 930	16.51 ± 1.29	0.00261
	1.13 μM	PPi	0.471	PPi	3.11 ± 0.52	7.70 ± 0.36	2.476
	0.74 μM			L-Valine	3955 ± 694	3.671 ± 0.198	0.00093
	0.74 μM			D-Isoleucine	4095 ± 394	4.169 ± 0.167	0.00102
ValRS	1.10 μM	L-Valine	14.4	L-Valine	12640 ± 1860	10.06 ± 0.87	0.00080
	1.10 μM	Ap_4A	1.53	Ap_4A	1940 ± 194	9.96 ± 0.426	0.00513
	1.10 μM	PPi	0.471	PPi	2.43 ± 2.13	4.71 ± 0.086	1.938

Figure 1

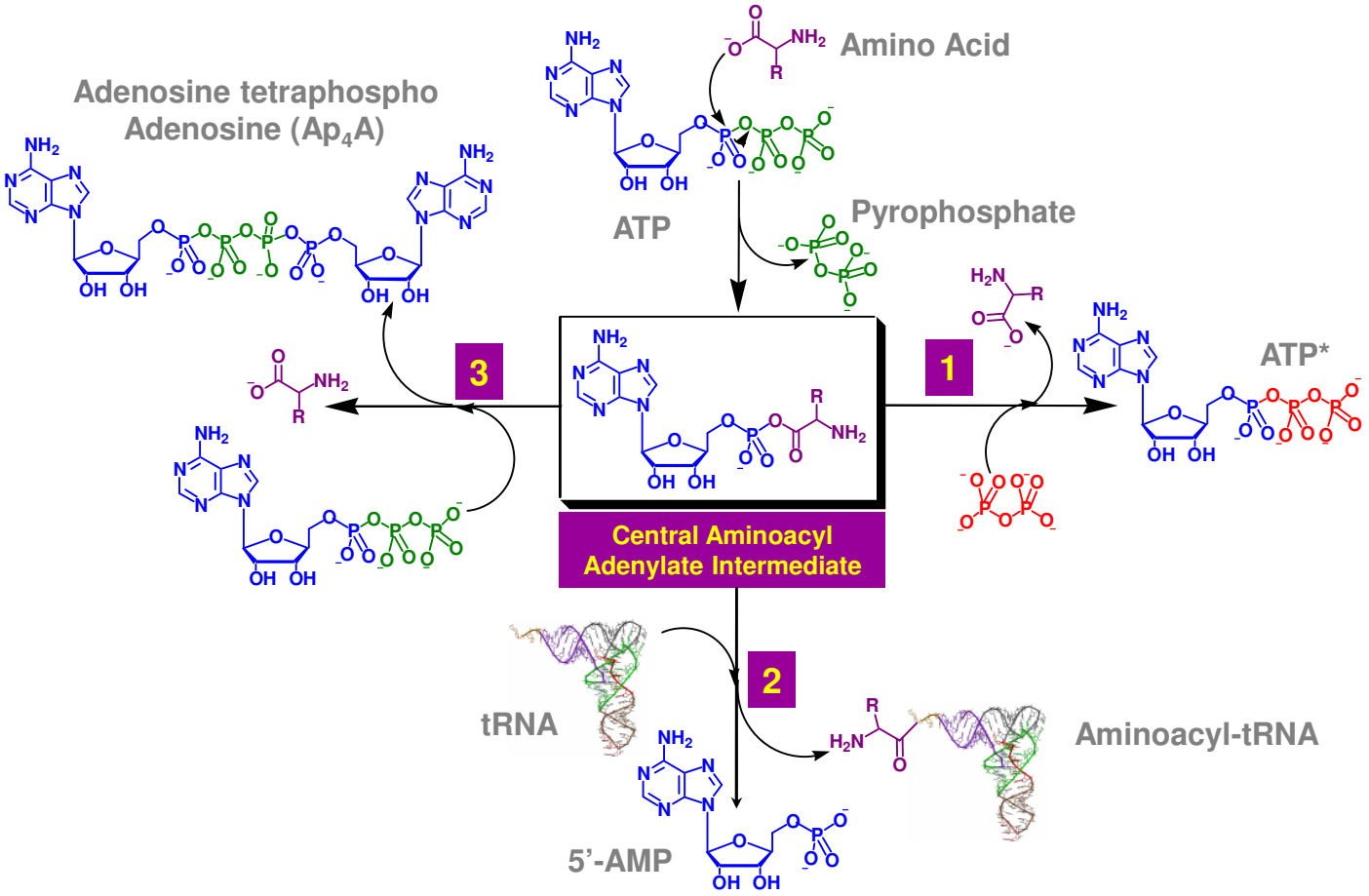
Amino Acid
Adenosine tetraphospho
Adenosine (Ap4A)
ATP
Pyrophosphate
ATP*
Central Aminoacyl
Adenylate Intermediate
1
2
3
tRNA
Aminoacyl-tRNA
5'-AMP

Figure 2

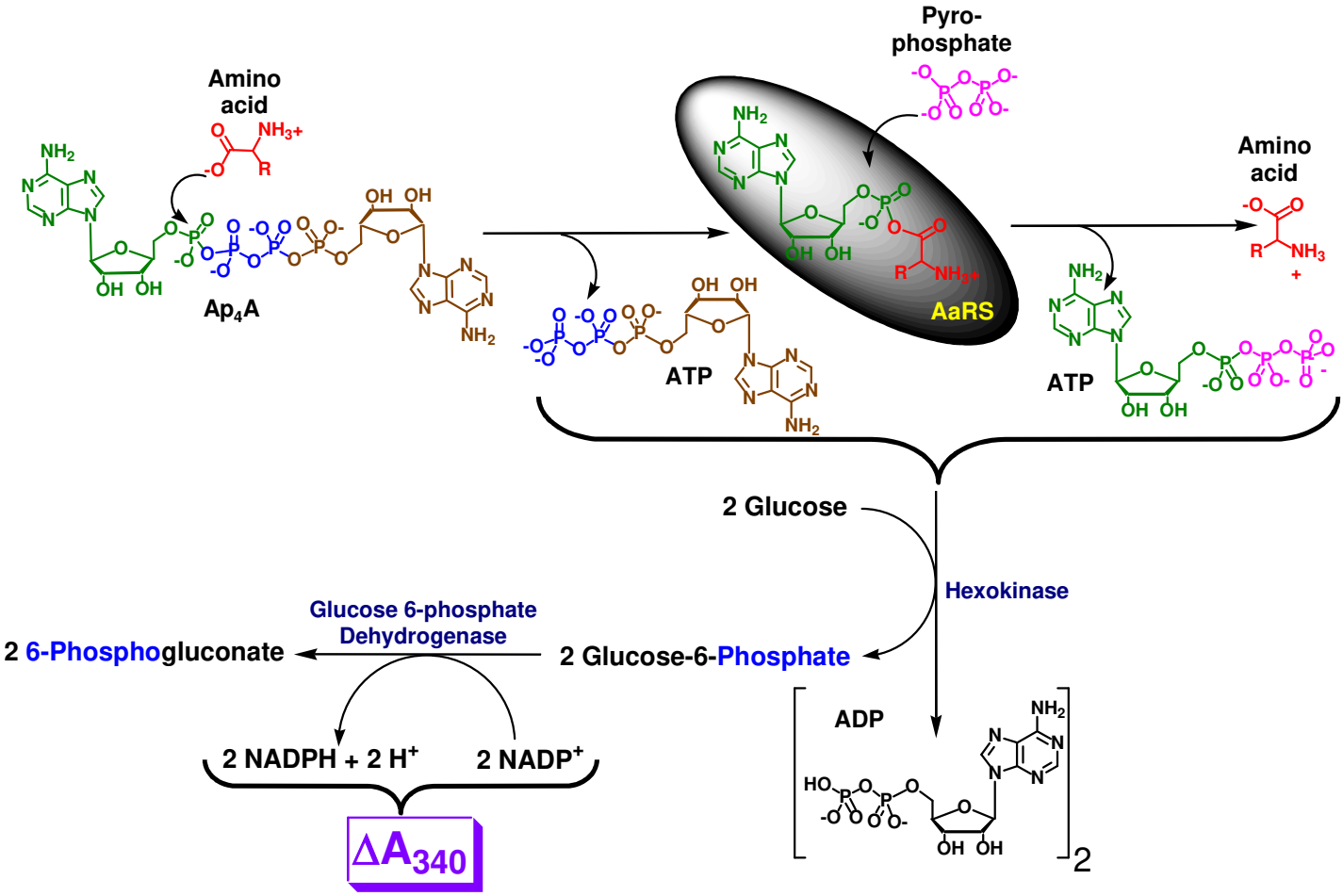
Amino acid
Ap4A
Pyro-phosphate
AaRS
ATP
Amino acid
ATP
2 Glucose
Hexokinase
Glucose 6-phosphate Dehydrogenase
2 6-Phosphogluconate
2 Glucose-6-Phosphate
ADP
2 NADPH + 2 H+
2 NADP+
ΔA340

Figure 3

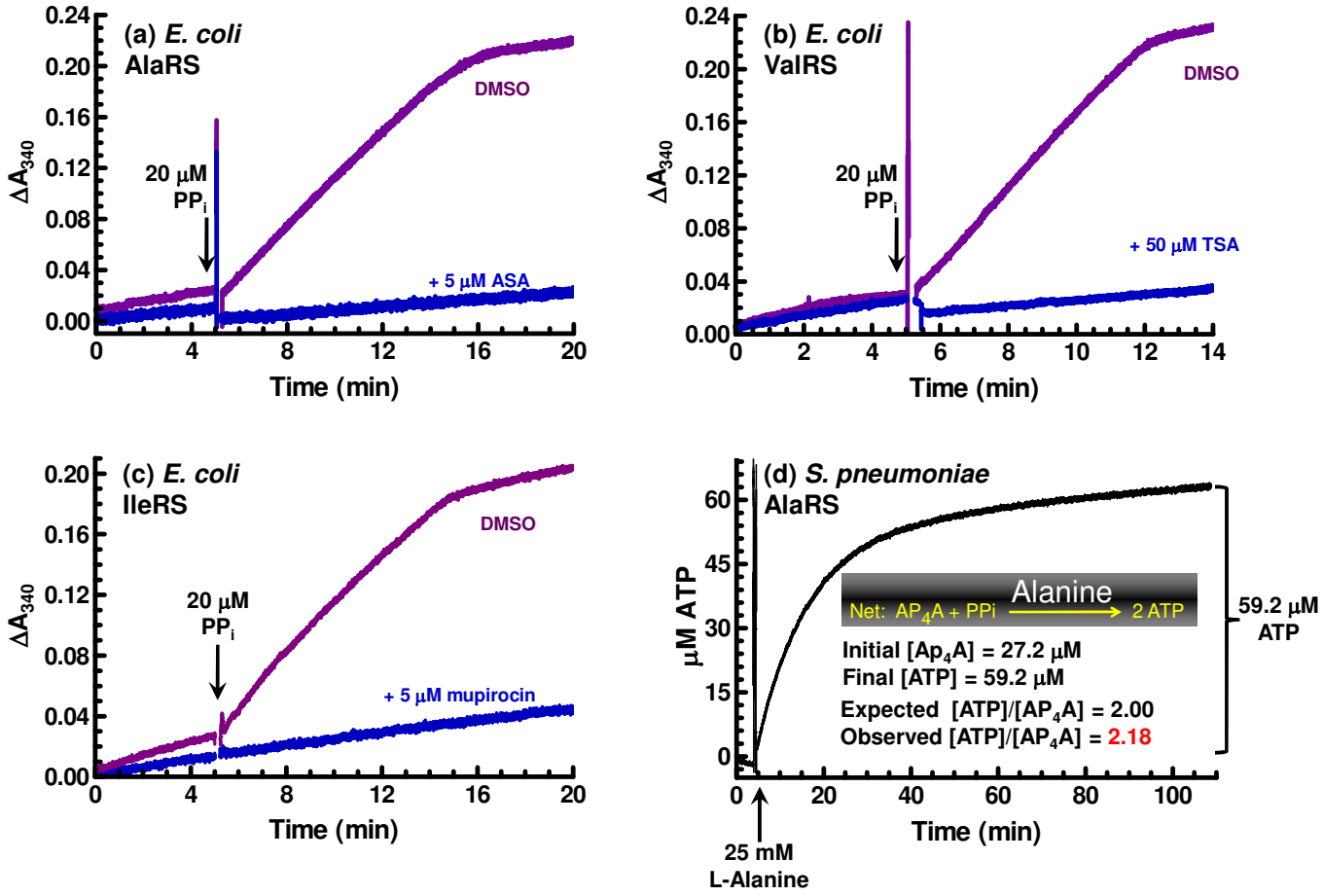
(a) E. coli
AlaRS
DMSO
20 µM
PPi
+ 5 µM ASA
ΔA340
Time (min)
(b) E. coli
ValRS
DMSO
20 µM
PPi
+ 50 µM TSA
ΔA340
Time (min)
(c) E. coli
IleRS
DMSO
20 µM
PPi
+ 5 µM mupirocin
ΔA340
Time (min)
(d) S. pneumoniae
AlaRS
Alanine
Net: AP4A + PPi → 2 ATP
Initial [Ap4A] = 27.2 µM
Final [ATP] = 59.2 µM
Expected [ATP]/[AP4A] = 2.00
Observed [ATP]/[AP4A] = 2.18
59.2 µM
ATP
µM ATP
Time (min)
25 mM
L-Alanine

Figure 4

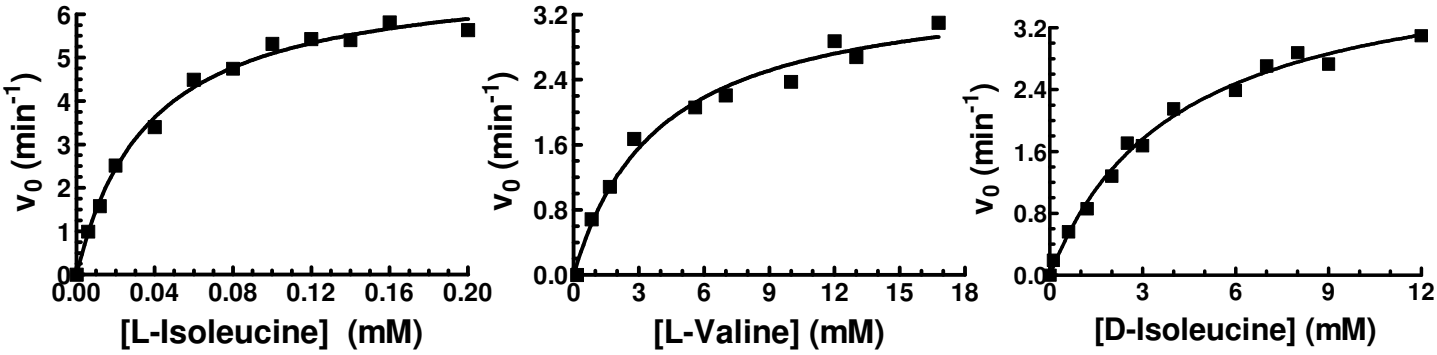
v0 (min-1)
[L-Isoleucine] (mM)
v0 (min-1)
[L-Valine] (mM)
v0 (min-1)
[D-Isoleucine] (mM)

Figure 5

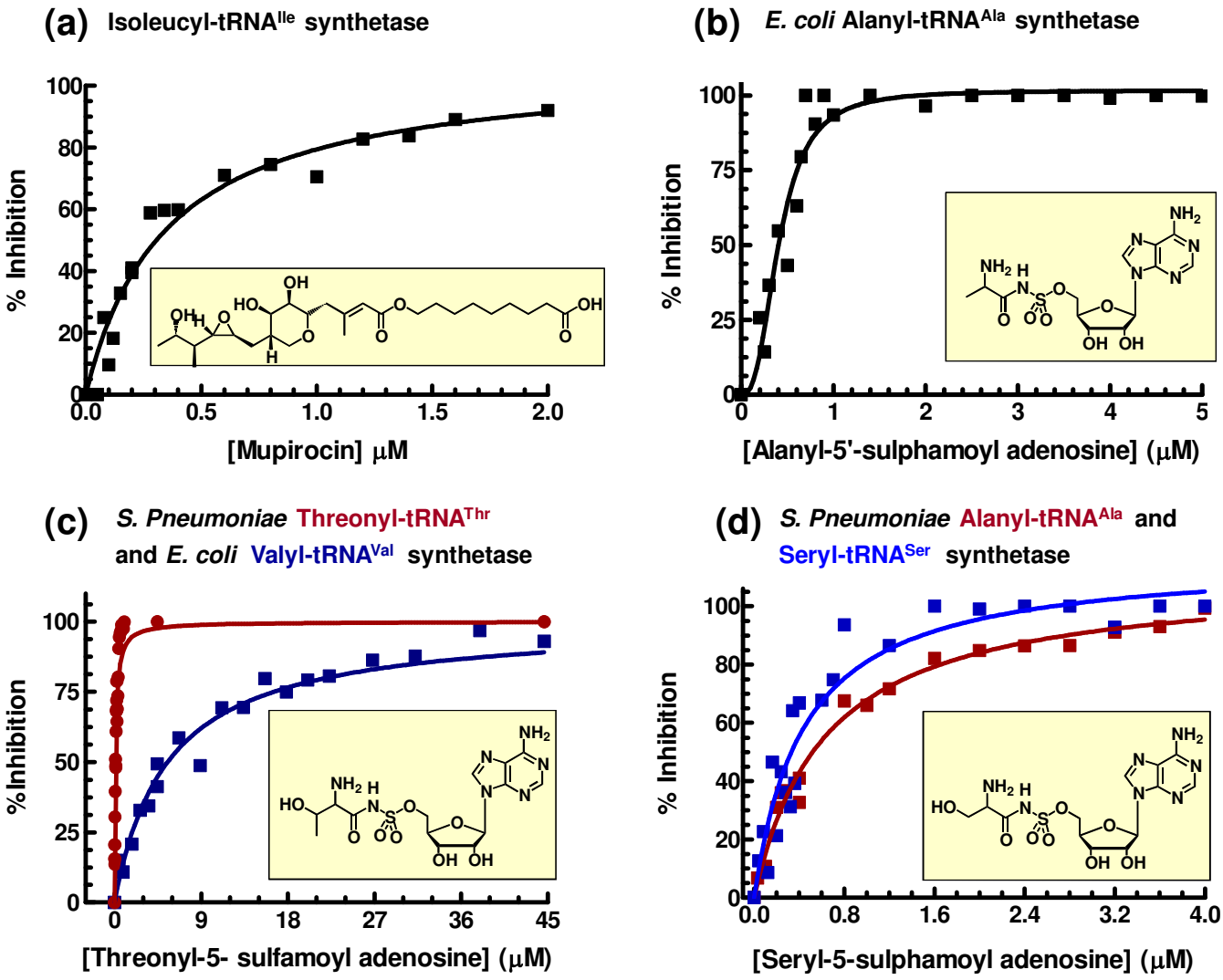
(a) Isoleucyl-tRNA^Ile synthetase
% Inhibition
[Mupirocin] μM
(b) E. coli Alanyl-tRNA^Ala synthetase
% Inhibition
[Alanyl-5'-sulphamoyl adenosine] (μM)
(c) S. Pneumoniae Threonyl-tRNA^Thr and E. coli Valyl-tRNA^Val synthetase
%Inhibition
[Threonyl-5- sulfamoyl adenosine] (μM)
(d) S. Pneumoniae Alanyl-tRNA^Ala and Seryl-tRNA^Ser synthetase
% Inhibition
[Seryl-5-sulphamoyl adenosine] (μM)

Figure 6

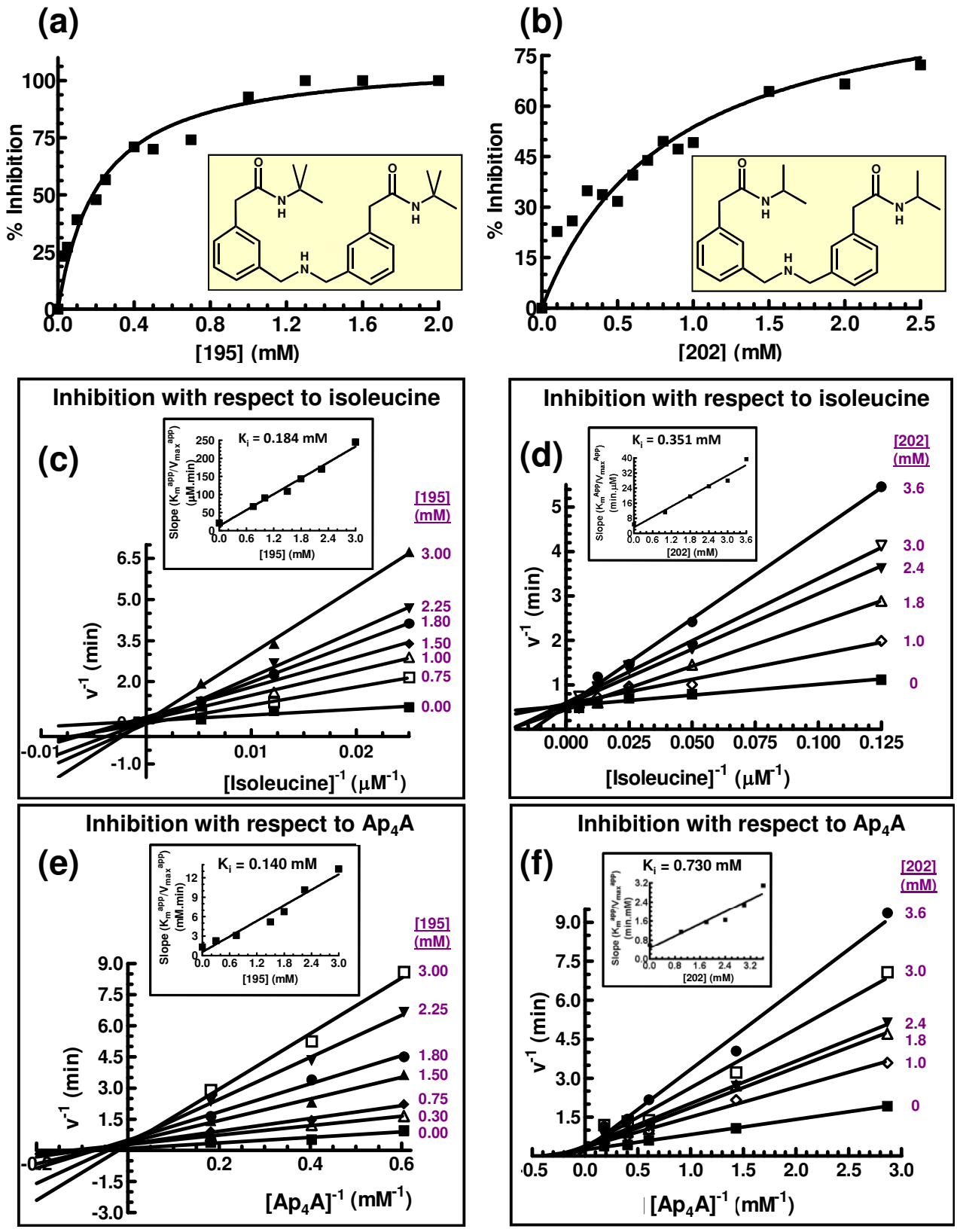
(a)
% Inhibition
[195] (mM)
(b)
% Inhibition
[202] (mM)
Inhibition with respect to isoleucine
(c)
Ki = 0.184 mM
Slope (Km app/Vmax app) (μM.min)
[195] (mM)
[195] (mM)
3.00
2.25
1.80
1.50
1.00
0.75
0.00
v-1 (min)
[Isoleucine]-1 (μM-1)
Inhibition with respect to isoleucine
(d)
Ki = 0.351 mM
Slope (Km App/Vmax App) (min.μM)
[202] (mM)
[202] (mM)
3.6
3.0
2.4
1.8
1.0
0
v-1 (min)
[Isoleucine]-1 (μM-1)
Inhibition with respect to Ap4A
(e)
Ki = 0.140 mM
Slope (Km app/Vmax app) (mM.min)
[195] (mM)
[195] (mM)
3.00
2.25
1.80
1.50
0.75
0.30
0.00
v-1 (min)
[Ap4A]-1 (mM-1)
Inhibition with respect to Ap4A
(f)
Ki = 0.730 mM
Slope (Km app/Vmax app) (min.mM)
[202] (mM)
[202] (mM)
3.6
3.0
2.4
1.8
1.0
0
v-1 (min)
[Ap4A]-1 (mM-1)

Figure 7

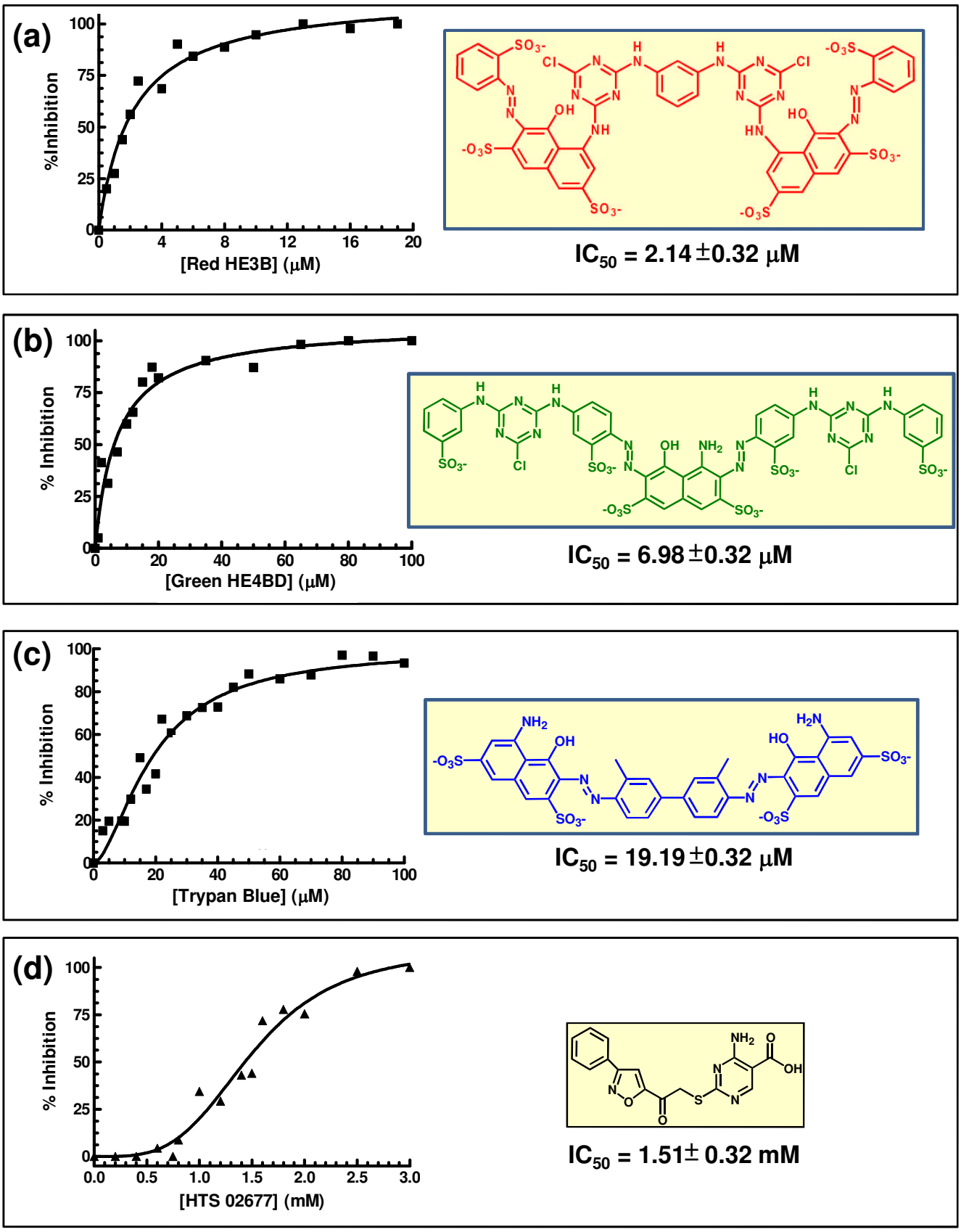
(a)
%Inhibition
[Red HE3B] (μM)
IC50 = 2.14 ±0.32 μM
(b)
% Inhibition
[Green HE4BD] (μM)
IC50 = 6.98 ±0.32 μM
(c)
% Inhibition
[Trypan Blue] (μM)
IC50 = 19.19 ±0.32 μM
(d)
% Inhibition
[HTS 02677] (mM)
IC50 = 1.51± 0.32 mM

Supporting Information

Adenosine Tetraphosphoadenosine Consumption Drives a Continuous ATP-Release Assay for Aminoacyl-tRNA Synthetase Catalysis

Adrian J. Lloyd[1*#], Nicola J. Potter[2#], Colin W.G. Fishwick[2], David I. Roper[1] and Christopher G. Dowson[1*]

[#]Both authors contributed equally to the manuscript.

[1]Department of Life Sciences, University of Warwick, Gibbet Hill Road, Coventry, West Midlands, CV4 7AL, UNITED KINGDOM and [2]School of Chemistry, University of Leeds, Leeds, LS2 9JT, UNITED KINGDOM.

*Correspondence: Adrian J. Lloyd email: Adrian.Lloyd@warwick.ac.uk and Christopher G. Dowson email: C.G.Dowson@warwick.ac.uk

Supporting Table Legend

Table S1: Characterization of the kinetics of substrate dependence of E. coli AlaRS, S. pneumoniae AlaRS and S. pneumoniae SerRS on the rate of pyrophosphorolysis of ADPNP

Supporting Figure Legends

Figure S1 Assay of AaRS activity by coupling pyrophosphate exchange in the presence of ADPNP: **(a)** ***Reaction scheme of the ADPNP assay*** where the AaRS catalyses the attack of the amino acid α-carboxyl on the α-phosphorus atom of ADPNP, forming an aminoacyl adenylate and liberating imidodiphosphate as the first product. Addition of pyrophosphate to the assay displaces the amino acid and forms ATP as a second product which can then be detected spectrophotometrically at 340 nm by coupling to

hexokinase and glucose 6 phosphate dehydrogenase. **(b)** ***Limited utility of ADPNP in the assay of AaRS pyrophosphate exchange.*** Time courses of the assay of ValRS, IleRS and SerRS in the ADPNP assay, where at time zero, all assays were constituted as described in Methods such that in the SerRS, IleRS and ValRS assays [ADPNP] was 0.1 mM, 1 mM and 1 mM respectively; [L-serine], [L-ilsoleucine] and [L-valine] were 0.4 mM, 2.4 mM and 2.5 mM respectively and [SerRS], [IleRS] and [ValRS] were 1.21 μM, 2.29 μM and 0.54 μM respectively. Background rates were monitored at 340 nm and assays were initiated by the addition of either 0.1 mM, 0.0834mM or 0.0834 mM pyrophosphate to the SerRS, IleRS and ValRS assays respectively at, **a**, **b** or **c** respectively.

Figure S2 Dependence of E. coli AlaRS, S. pneumoniae AlaRS and SerRS on ADPNP, pyrophosphate and cognate amino acid. All assays were executed as described in Methods, where assays were initiated with pyrophosphate and initial velocity (v_0) was obtained from the difference of rates obtained post and pre-addition of pyrophosphate. When held constant, the concentrations of pyrophosphate, ADPNP and L-amino acid were as reported in Table S1. For all determinations of dependence of v_0 on [substrate], the [enzyme] is recorded in Table S1. ***Panel*** ***a*** **–** ***c*** ***:*** Dependence of *S. pneumoniae* SerRS on [pyrophosphate], [ADPNP] and [L-serine]; ***Panel*** ***d*** **–** ***f*** ***:*** Dependence of *S. pneumoniae* AlaRS on [pyrophosphate], [ADPNP] and [L-alanine]; ***Panel*** ***g*** **–** ***i*** ***:*** Dependence of *E. coli* AlaRS on [pyrophosphate], [ADPNP] and [L-alanine]. Kinetic constants were determined by non-linear regression and are recorded in Table S1.

Figure S3 Dependence of E. coli AlaRS, IleRS and ValRS on Ap_4A, pyrophosphate and cognate amino acid. All assays were executed as described in Methods, where assays were initiated with pyrophosphate and v_0 was obtained from the difference of rates obtained post and pre-addition of pyrophosphate. When held constant, the concentrations of pyrophosphate, Ap_4A and L-amino acid were as reported in Table 1. For all determinations of dependence of v_0 on [substrate], the [enzyme] is recorded in Table 1. ***Panel*** ***a*** **–** ***c*** ***:***

Dependence of IleRS on [pyrophosphate], [Ap_4A] and [L-isoleucine]; ***Panel – :*** Dependence of *ValRS* on [pyrophosphate], [Ap_4A] and [L-valine]; ***Panel g – i :*** Dependence of *E. coli* AlaRS on [pyrophosphate], [Ap_4A] and [L-alanine]. Kinetic constants were determined by non-linear regression and are recorded in Table 1.

Figure S4 Time course of S. pneumoniae AlaRS catalysed pyrophosphorolysis of Ap_4A with non-cognate L-serine. Assay was as outlined in Methods, where the final concentrations of AlaRS, L-serine, Ap4A and pyrophosphate were 0.70 μM, 10 mM, 2 mM and 0.471 mM respectively. All components except AlaRS and L-serine were present at time zero. *S. pneumoniae* AlaRS and L-serine were added as indicated. Progress of the reaction was followed at 340 nm.

Figure S5 Inhibition of AaRSs by aminoacyl-sulphamoyl adenylates: (a) Inhibition of S. pneumoniae ThrRS by seryl sulphamoyl adenosine. Figure shows ThrRS rates in the presence of increasing [seryl-5'-sulphamoyl adenosine] (abbreviated to SSA in figure). Assays were carried out as described in Methods, where [pyrophosphate], [ADPNP], [L-threonine] were 0.471 mM, 0.254 mM and 10 mM respectively. [ThrRS] was at 0.55 μM. Background data were collected until 2.4 min, when the assays were initiated by the addition of L-threonine (arrow). Assays were performed in the presence of 0, 5 μM, 50 μM and 500 μM seryl-5'-sulphamoyl adenosine. The % inhibition caused by increasing seryl-5'-sulphamoyl adenosine is recorded adjacent to the traces as % I. ***(b) Specificity of inhibition displayed by SerRS for seryl-5'-sulphamoyl adenosine compared to alanyl-5'-sulphamoyl adenosine.*** Figure shows aminoacyl-specificity of inhibition of *S. pneumoniae* SerRS by cognate seryl-5'-sulphamoyl adenosine and non-cognate alanyl-5'-sulphamoyl adenosine. Assays were performed as described in Methods where [pyrophosphate], [ADPNP] and [L-serine] were 1 mM, 0.250 mM and 0.2 mM respectively. [SerRS] was at 2.08 μM. Assays were initiated by the addition of L-serine and performed at

concentrations of alanyl-5'-sulphamoyl adenosine (red) and seryl-5'-sulphamoyl adenosine (blue).

Table S1

AaRS	Species	$[AaRS]_{Assay}$	Nonvaried substrate	[Nonvaried substrate] (mM)	Varied Substrate	K_m^{App} (μM)	k_{cat}^{App} (min^{-1})	K_{cat}^{App}/k_m^{App} ($min^{-1}.\mu M^{-1}$)
AlaRS	*E. coli*	0.37 μM	L-Alanine	0.200	L-Alanine	1418 ± 68	78.24 ± 1.14	0.0552
		0.92 μM	ADPNP	0.243	ADPNP	4.8 ± 0.64	9.384 ± 0.24	1.955
		0.92 μM	PPi	0.471	PPi	24.89 ± 2.66	7.038 ± 0.24	0.283
	S. pneumoniae	0.21 μM	L-Alanine	0.200	L-Alanine	1770 ± 220	118.2 ± 3.0	0.0667
		0.21 μM	ADPNP	0.254	ADPNP	12.82 ± 1.77	13.26 ± 0.48	1.030
		0.17 μM	PPi	0.471	PPi	22.68 ± 2.78	13.20 ± 0.72	0.582
SerRS	*S. pneumoniae*	2.08 μM	L-Serine	0.200	L-Serine	527 ± 64	1.86 ± 0.06	0.0035
		12.14 μM	ADPNP	0.254	ADPNP	107.2 ± 12.7	0.467 ± 0.0074	0.0044
		12.14 μM	PPi	0.471	PPi	56.35 ± 6.96	0.420 ± 0.018	0.0075

Figure S1a

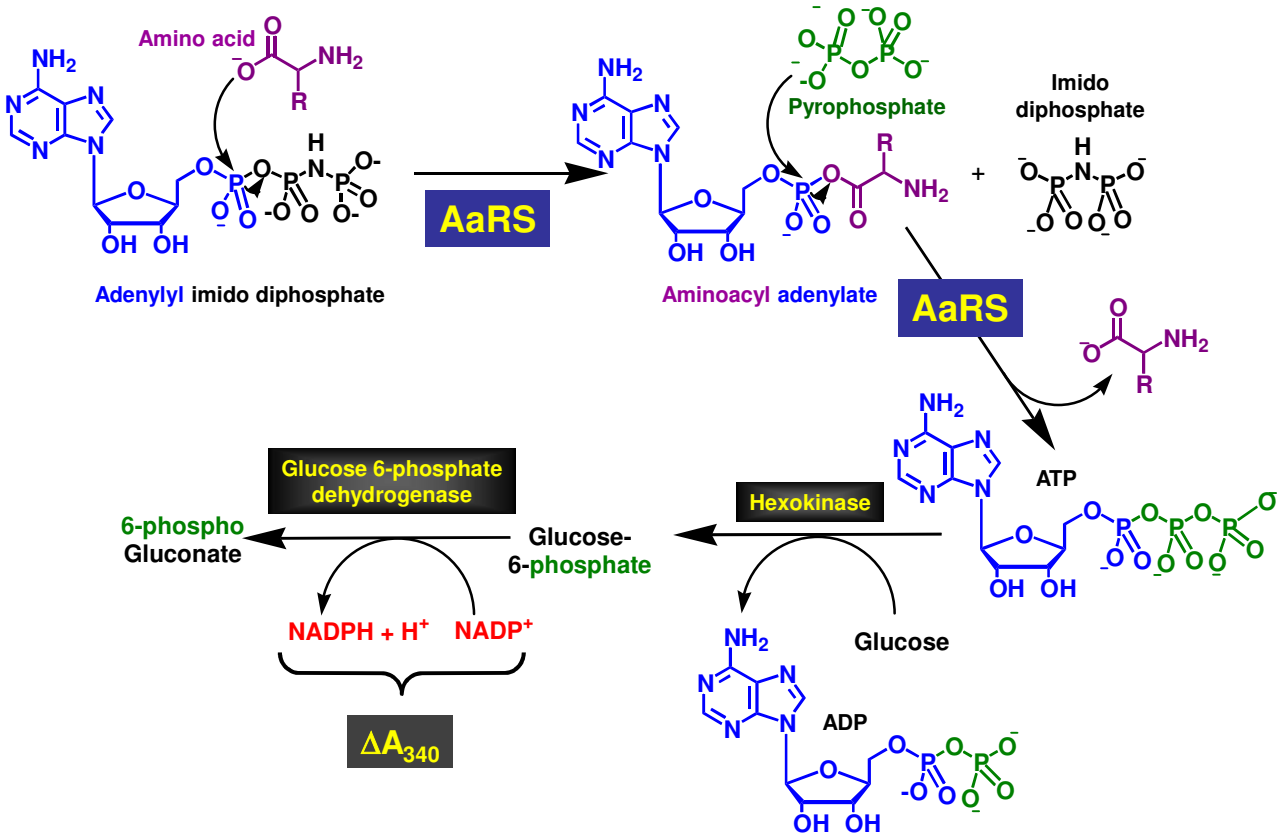

Figure S1b

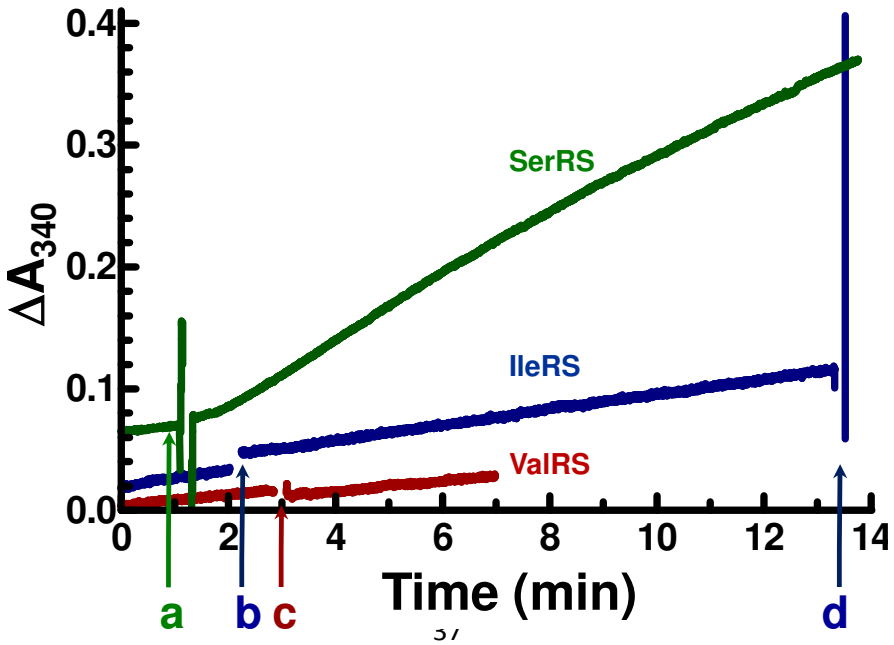

Figure S2

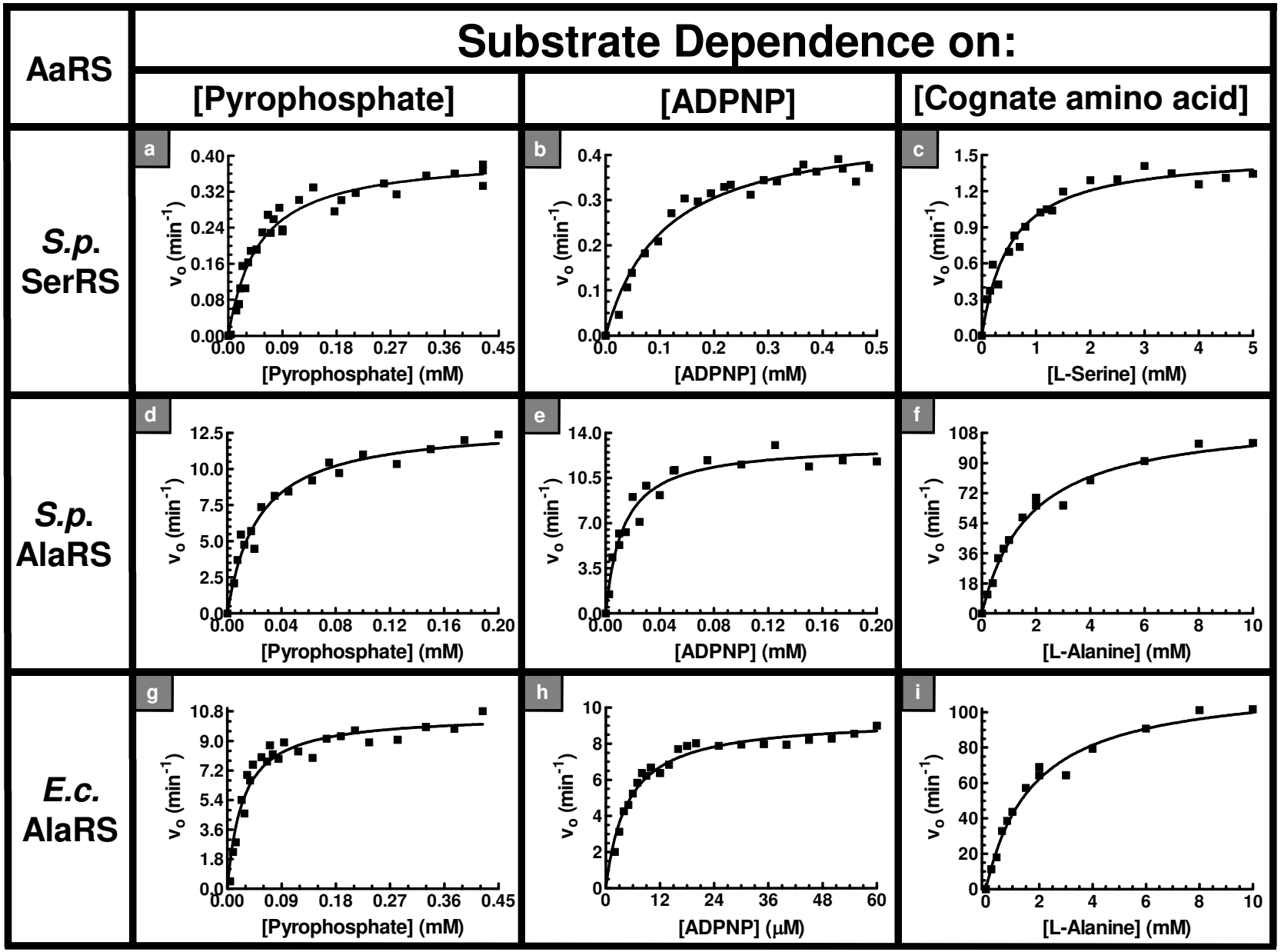
AaRS
Substrate Dependence on:
[Pyrophosphate]
[ADPNP]
[Cognate amino acid]
S.p. SerRS
S.p. AlaRS
E.c. AlaRS
a
b
c
d
e
f
g
h
i
v_o (min^-1)
[Pyrophosphate] (mM)
[ADPNP] (mM)
[L-Serine] (mM)
[L-Alanine] (mM)
[ADPNP] (μM)

Figure S3

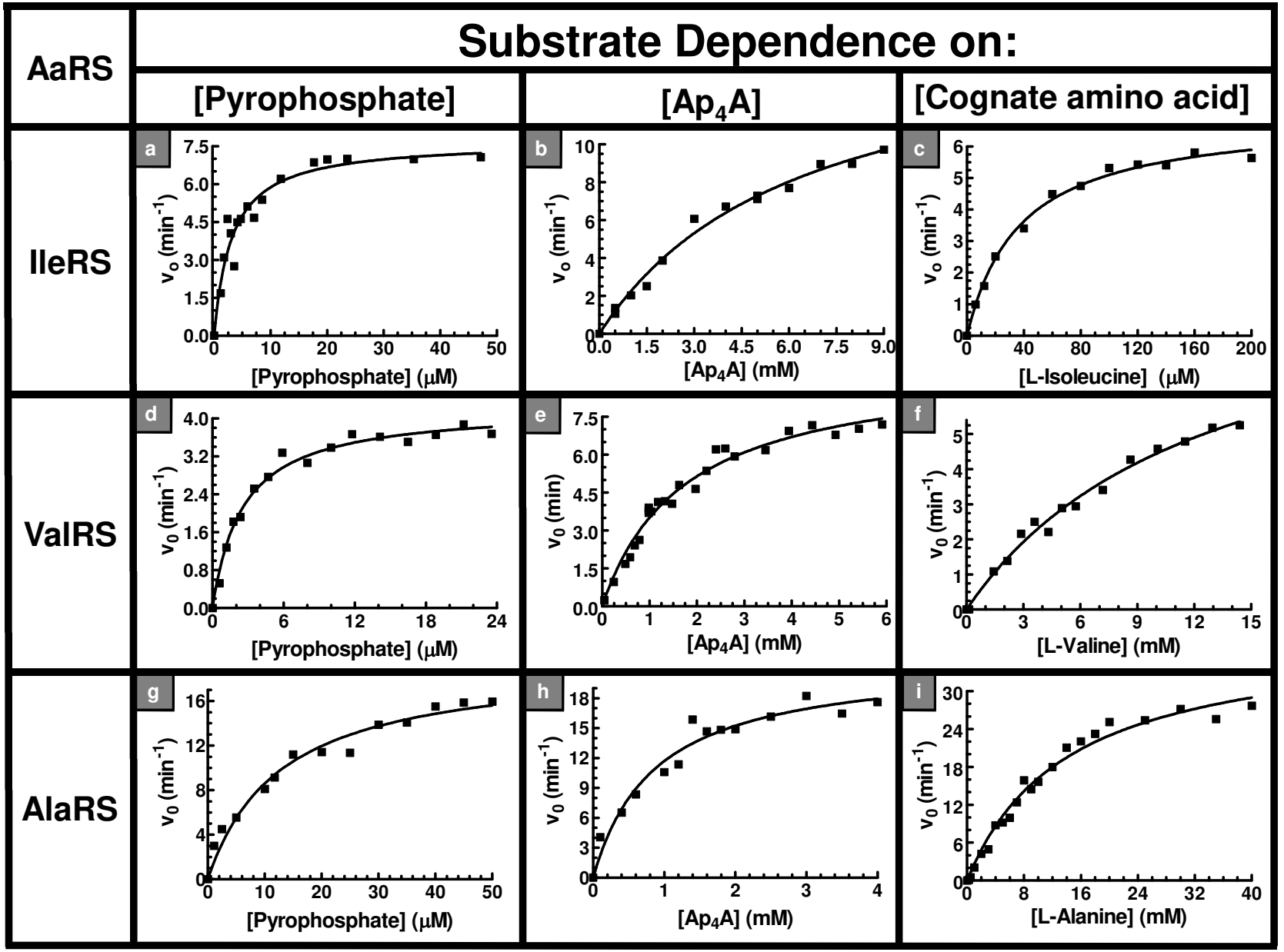
AaRS
Substrate Dependence on:
[Pyrophosphate]
[Ap4A]
[Cognate amino acid]
IleRS
ValRS
AlaRS
a
b
c
d
e
f
g
h
i
v0 (min-1)
v0 (min)
[Pyrophosphate] (μM)
[Ap4A] (mM)
[L-Isoleucine] (μM)
[L-Valine] (mM)
[L-Alanine] (mM)

Figure S4

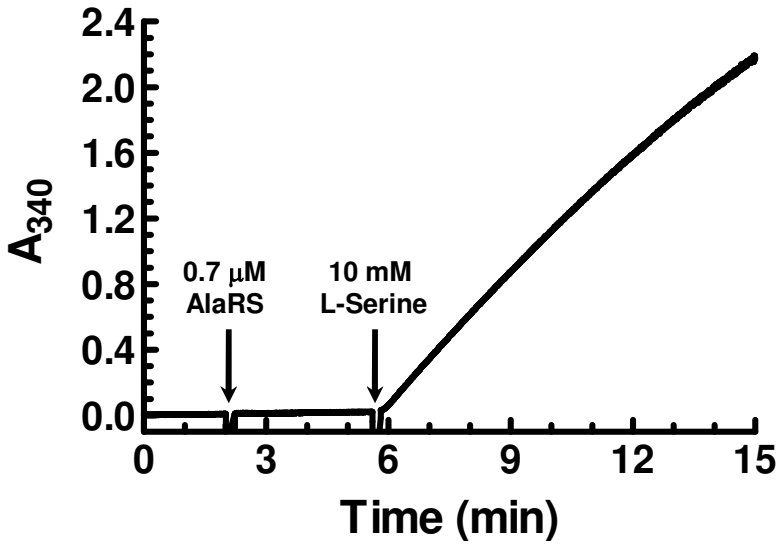
2.4
2.0
1.6
1.2
0.8
0.4
0.0
A340
0.7 μM
AlaRS
10 mM
L-Serine
0
3
6
9
12
15
Time (min)

Figure S5a

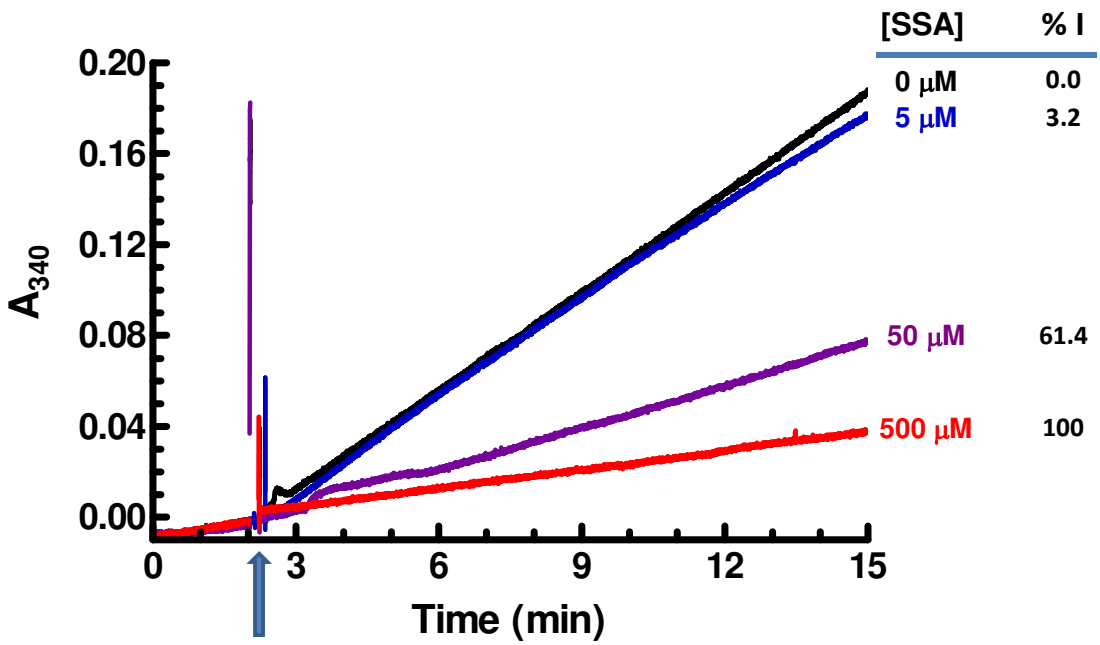

Figure S5b